

## Biophysical Feature, Crystallization and X-ray Crystallographic Studies of *Toxascaris leonina* Galectin

Minkyung Sung,<sup>a</sup> Mi Suk Jeong,<sup>a</sup> Woo Chul Lee,<sup>†</sup> Jeong Hyun Song,<sup>†</sup> Hye Yeon Kim,<sup>†</sup>  
Min Kyoung Cho,<sup>‡</sup> Hak Sun Yu,<sup>‡</sup> and Se Bok Jang<sup>\*</sup>

*Department of Molecular Biology, College of Natural Sciences, Pusan National University, Busan 609-735, Korea*

*<sup>†</sup>Division of Magnetic Resonance, Korea Basic Science Institute, Chungbuk, Korea*

*<sup>‡</sup>Department of Parasitology, School of Medicine, Pusan National University, Gyeongsangnam-do 626-870, Korea*

*\*E-mail: sbjang@pusan.ac.kr*

*Received September 26, 2011, Accepted November 21, 2011*

Galectins are generally believed to be potential candidates for use in the development of novel anti-inflammatory agents or as selective modulators of the immune response. In particular, galectin-9 exhibits some of the extracellular functions, including cell aggregation, adhesion, chemoattraction, activation, and apoptosis. Tl-galectin (Tl-gal, galectin-9 homologue gene) was isolated from an adult worm of the *Toxascaris leonina*. The full-length Tl-gal gene, which was incorporated into pET-28a, was overexpressed in *E. coli* and purified by nickel affinity and gel filtration chromatographies. The purified Tl-gal was crystallized using the hanging-drop vapor-diffusion method. The crystal belonged to the tetragonal space group  $P4_1$ , with unit-cell parameters of  $a = b = 75.7 \text{ \AA}$  and  $c = 248.4 \text{ \AA}$ . The crystals were obtained at  $20 \text{ }^\circ\text{C}$  and diffracted to a resolution of  $3.0 \text{ \AA}$ . The asymmetric unit contained four molecules of Tl-gal, which gave a crystal volume per protein mass ( $V_m$ ) of  $2.8 \text{ \AA}^3 \text{ Da}^{-1}$  and a solvent content of 54.1%.

**Key Words** : Crystallization, X-ray analysis, *Toxascaris leonina*, Galectin

### Introduction

Infection with gastrointestinal nematodes is prevalent worldwide, despite the fact that *anti*-helminthic medications are regarded as safe, efficient, and widely available globally. In recent years, the effect of parasitic infection on the incidence of allergic and autoimmune diseases, such as Crohn's disease, has been receiving an increased amount of attention.<sup>1</sup> Long-lived helminthic parasites are remarkable in their ability to down-regulate host immunity, protect themselves from elimination, and minimize severe pathological host changes.<sup>2</sup> Helminths can prevent and reverse intestinal inflammation in animal models of inflammatory bowel disease.<sup>3</sup> Current therapeutic strategies aim to modify the inflammatory responses in affected individuals and minimize injury to the intestines.<sup>4</sup> Several immune down-regulatory molecules from parasites have already been isolated and identified as mammal cytokine homologues, protease inhibitors, abundant larval transcript antigens, glyco-networks, and venom allergen-like proteins.<sup>5-11</sup>

Galectins are members of a large, growing family of animal lectins, which are highly conserved throughout animal evolution. They have been shown to affect different functions relevant to innate and adaptive immuneresponses.<sup>12</sup> Some of the extracellular functions thus far reported for galectins include developmental processes activation, cell adhesion, chemotaxis, cell-growth regulation, and apoptosis. Galectins are generally believed to be potential candidates

for use in the development of novel *anti*-inflammatory agents or as targets for *anti*-inflammatory drugs.<sup>13</sup>

A galectin-9 homologue gene was previously isolated from an adult worm of the canine gastrointestinal nematode parasite, *Toxascaris leonina*, via random cDNA library sequencing.<sup>2</sup> The clinical symptoms of dextran sulfate sodium-treated mice after recombinant Tl-gal pre-treatment were found to be minimized, or less profound, when compared to those of the Tl-gal untreated group. In addition, the Tl-gal treated group exhibited significantly increased levels of TGF- $\beta$  and IL-10 ( $p < 0.05$ ).<sup>1</sup> Interleukin (IL)-10 is a regulatory cytokine that inhibits macrophage and dendritic cell activation and suppresses production of proinflammatory mediators such as tumor necrosis factor  $\alpha$ , IL-12, IL-1, nitric oxide, and several chemokines.<sup>14</sup> Transforming growth factor (TGF)- $\beta$  prevents naive T cells from expressing transcription factors (T-bet, Gata-3) that drive their development into effector T cells.<sup>15</sup> Instead, TGF- $\beta$  induces T cells to express the transcription factor Foxp3 (scurfin), which drives their development into a regulatory phenotype.<sup>16</sup> Similar to the host galectin, Tl-gal may function as a regulatory molecule in the host immune system.

Galectins constitute a family of structurally related  $\beta$ -galactoside-binding proteins, which are defined by their affinity for poly-*N*-acetyllactosamine-enriched glycoconjugates and sequence similarities in the carbohydrate recognition domain. Until now, there have been no reports on the X-ray structure of Tl-gal. The purified full-length galectin from *Toxascaris leonina* grew into a suitable crystal for X-ray crystallographic analysis, and the crystal structure was deter-

<sup>‡</sup>These authors contributed equally to this work.

mined at a resolution of 3.0 Å. In this study, we evaluated the biophysical feature, crystallization behavior, and crystallographic properties of the Tl-gal protein in *E. coli*. This structural information will provide insights into the design of novel regulatory molecules for the treatment of inflammatory, allergic or immune diseases.

### Experimental

**Protein Expression and Purification.** The full-length Tl-gal gene was incorporated into plasmid pET-28a (Novagen), which has strong T7 transcriptional and translational sequences. The Tl-gal construct was transformed into the expression host *E. coli* BL21(DE3). A single colony was inoculated in 5 mL LB (Luria-Bertani) medium enriched with 10 µg/mL kanamycin. Following overnight culture at 37 °C, bacterial cells were added to the 1 L of LB containing antibiotics kanamycin and the cultures were maintained at 37 °C until the OD<sub>600</sub> reached 0.5. Protein expression was induced by adding 0.5 mM of isopropyl β-D-thiogalactopyranoside (IPTG). The bacterial cells were induced for 16 h at 20 °C, and then harvested by centrifugation at 3,660 × g for 25 min. The resulting cell pellets were either used immediately or frozen at -70 °C. The cell pellets were resuspended with lysis buffer A [50 mM Tris-HCl (pH 7.5), 200 mM NaCl] and disrupted by sonication on ice. Subsequently, cell lysates were centrifuged at 20,170 × g for 45 min to remove unbroken cells and debris. Soluble Tl-gal supernatant was loaded onto a Ni-NTA (Amersham-Pharmacia Biotech) column that had been pre-equilibrated with buffer A. The column was washed with buffer A containing 20 mM imidazole at a flow rate of 2 mL/min, and the bound protein was eluted using buffer A containing 200 mM imidazole. Purified fractions of the Tl-gal protein from Ni-NTA column were mixed and purified by gel-filtration chromatography. A concentrated fraction was injected using a pump. Gel filtration was performed by FPLC using a Superdex 200 10/300 GL column (Amersham-Pharmacia Biotech) equilibrated in buffer A. The flow rate of the mobile phase was 0.4 mL/min, and the fractions were collected. All purification steps were assessed by SDS-PAGE using 12 and 15% polyacrylamide gels and Coomassie blue staining.

**MALDI-TOF Mass Analysis.** For in-gel digestion, 10 µL of trypsin solution [2 ng/L of trypsin in 25 mM ammonium bicarbonate (pH 8.0)] was added and kept overnight at 37 °C. Peptides were extracted with 50% CAN/1% TFA (trifluoroacetic acid) and dried in a vacuum desiccator overnight, followed by reconstitution with 3 µL of CHCA (α-Cyano-4-hydroxy-cinnamic acid) matrix solution (8 mL of CHCA in 1 mL of 50% CAN/1% TFA). One microliter of sample was loaded onto a 96 × 2 MALDI plate. The peptide mass was acquired using a Voyager DE-PRO (Applied Biosystems, Framingham, MA) in reflector mode under an accelerating voltage of 20,000 V, grid voltage of 76% and guidewire voltage of 0.002%. The Cal Mix 2 of the MALDI-TOF MS calibration kit (Applied Biosystems, Framingham,

MA) was used for external calibration. Autolysis fragments of trypsin were used for internal calibration. Peptide matching and protein identification were carried out using the Mascot peptide mass fingerprint. The sequences of the digested peptides were matched with the protein sequences in the database using the MASCOT program.

**Circular Dichroism (CD) and Temperature Controller Measurements.** Circular dichroism measurements were acquired using a spectropolarimeter (JASCO J-815) in a 0.1 cm cell at 0.2 nm intervals and 25 °C. The CD spectra of the purified Tl-gal protein were recorded in the range of 190-260 nm. Each spectrum was the average of 10 scans. Far-UV CD spectra were acquired at a protein concentration of 0.5 mg/mL. The CD spectra were obtained in milli-degrees and were converted to molar ellipticity prior to secondary structure analysis using the CDNN program.<sup>17</sup> Temperature controller spectra were captured using the same set-up by heating the proteins with a constant temperature gradient from 20 to 60 °C. The CD spectra of the proteins were obtained at various pH levels, which were adjusted using different buffers.

**Differential Scanning Calorimetry (DSC).** Differential scanning calorimetric measurements were carried out on a DSC 204 F1 (NETZSCH DSC, USA). About 1 mg of protein was placed in an aluminum pan, which was then immediately sealed. The pan was heated to -10 - 90 °C at a rate of 1 °C/min. An empty pan was used as a reference. The sensitivity was 0.1 µw and the sensor time constant was 0.6. The reference was in the same state (liquid) and was placed in a reference crucible made of aluminum. The onset temperature (T<sub>m</sub>), peak transition or denaturation temperature (T<sub>d</sub>), enthalpy of denaturation (ΔH) and cooperativity, as represented by the width at half-peak height (ΔT<sub>1/2</sub>), were computed from the thermograms using Universal Analysis Version 3.0.3. The sample was examined twice by repeating the heating-cooling cycles. The sealed pan containing the protein sample and reference was equilibrated.

**UV-vis Absorption.** Absorbance measurements were carried out using a Shimadzu UV-1650 PC UV-vis Spectrophotometer with 1.0-cm quartz cells. The UV absorbance spectra of the Tl-gal were obtained using concentrations of 0.5 mg/mL. Thermal unfolding were performed using the same set up buffer A. To examine the effect of temperature condi-

**Table 1.** Crystallographic Statistics

Space group	<i>P4</i> <sub>1</sub>
Unit cell parameters	a = 75.70 Å b = 75.70 Å c = 248.38 Å
Resolution (Å)	30.0-3.0
Completeness (%) (3.16-3.0 Å)	80.3 (79.4)
Observed reflections	294,380
Unique reflections	24,478
<i>I</i> /σ ( <i>I</i> )	7.3 (1.8)
R <sub>merge</sub> (%)	8.7 (39.8)

Values in parentheses are for the highest resolution shell.

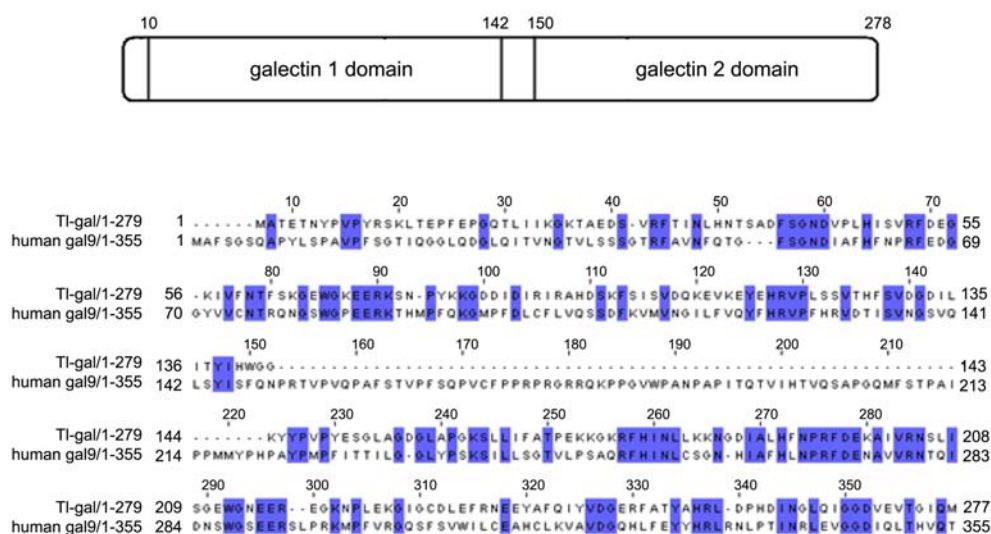


**Figure 1.** Schematic diagram showing the domain structure of full-length Tl-gal and sequence alignment of Tl-gal with human galectin-9. The residues conserved across 2 species are colored in blue.

tions, the Tl-gal samples were incubated at various temperatures (20 °C to 60 °C) for 5 min. pH-dependent unfolding studies were carried out under various pH (pH 5.5-9.5). The UV spectra of the Tl-gal were recorded in the 285-295 nm range.

**Crystallization.** Crystallization was performed by the hanging-drop vapor-diffusion method using the crystallization screening kit (Hampton Research) at 293 K. A

hanging drop was prepared by mixing equal volumes (1.0  $\mu$ L each) of the protein solution and the reservoir solution. Crystals were grown using a reservoir of 30% polyethylene glycol-400 with 0.1 M CHES buffer at pH 9.5. Under these conditions, crystals appeared after about 3 days and the crystals grew to maximum size within two weeks.

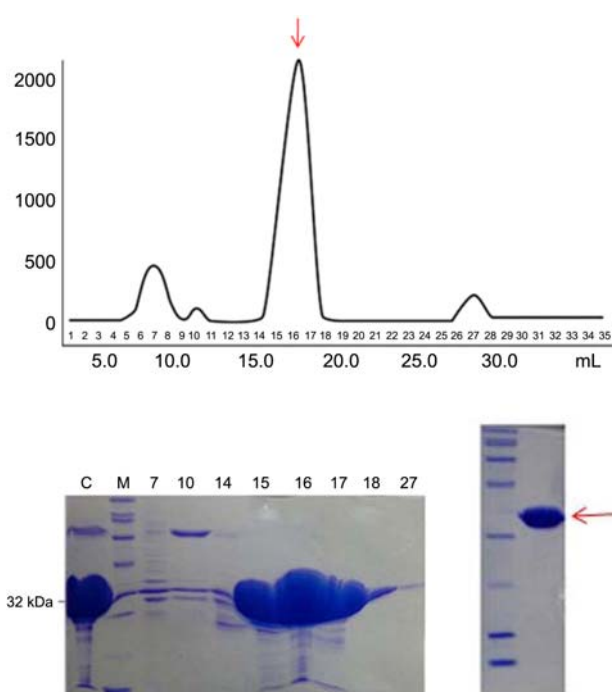


**Figure 2.** Purification of Tl-gal. After the protein was purified using Ni-NTA affinity chromatography, eluted fractions were concentrated and purified again by gel-filtration chromatography. (a) Gel filtration profile of the Tl-gal and SDS-PAGE of the fractions. The protein peaks are shown with the arrows. (b) Gel-filtration chromatography. C: control, M: protein molecular marker, each number of fractions are marked.

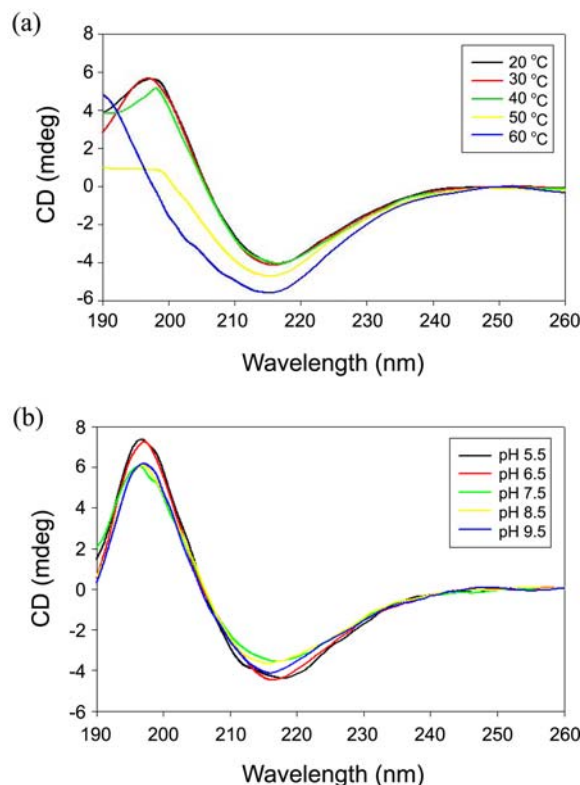


**Figure 3.** Far-UV CD spectra of the Tl-gal protein. (a) CD spectra of the Tl-gal protein at different temperatures (20-60 °C). (b) Effects of pH (5.5-9.5) on the CD spectra of Tl-gal. The CD spectrum was measured from 190 to 260 nm, and the CD signal was merged into CDNN. These spectra were the result of 10 scans.

**Data Collection and Analysis.** The Tl-gal was collected on beamline 5A at the Photon Factory (Tsukuba, Japan). Before data collection, the crystal was soaked briefly in a cryoprotectant solution, which was the precipitant solution containing 20% glycerol. Diffraction data were obtained and processed using the programs *MOSFLM* and *SCALEPACK* (Table 1).<sup>18,19</sup>

## Results and Discussion

The sequence of the Tl-gal gene had a 35% identity with the human galectin-9 gene. The amino acid sequences were aligned using Jalview (Fig. 1). The Tl-gal construct was overexpressed in *Escherichia coli* BL21 (DE3) and protein expression was induced with 0.5 mM IPTG at 37 °C. As

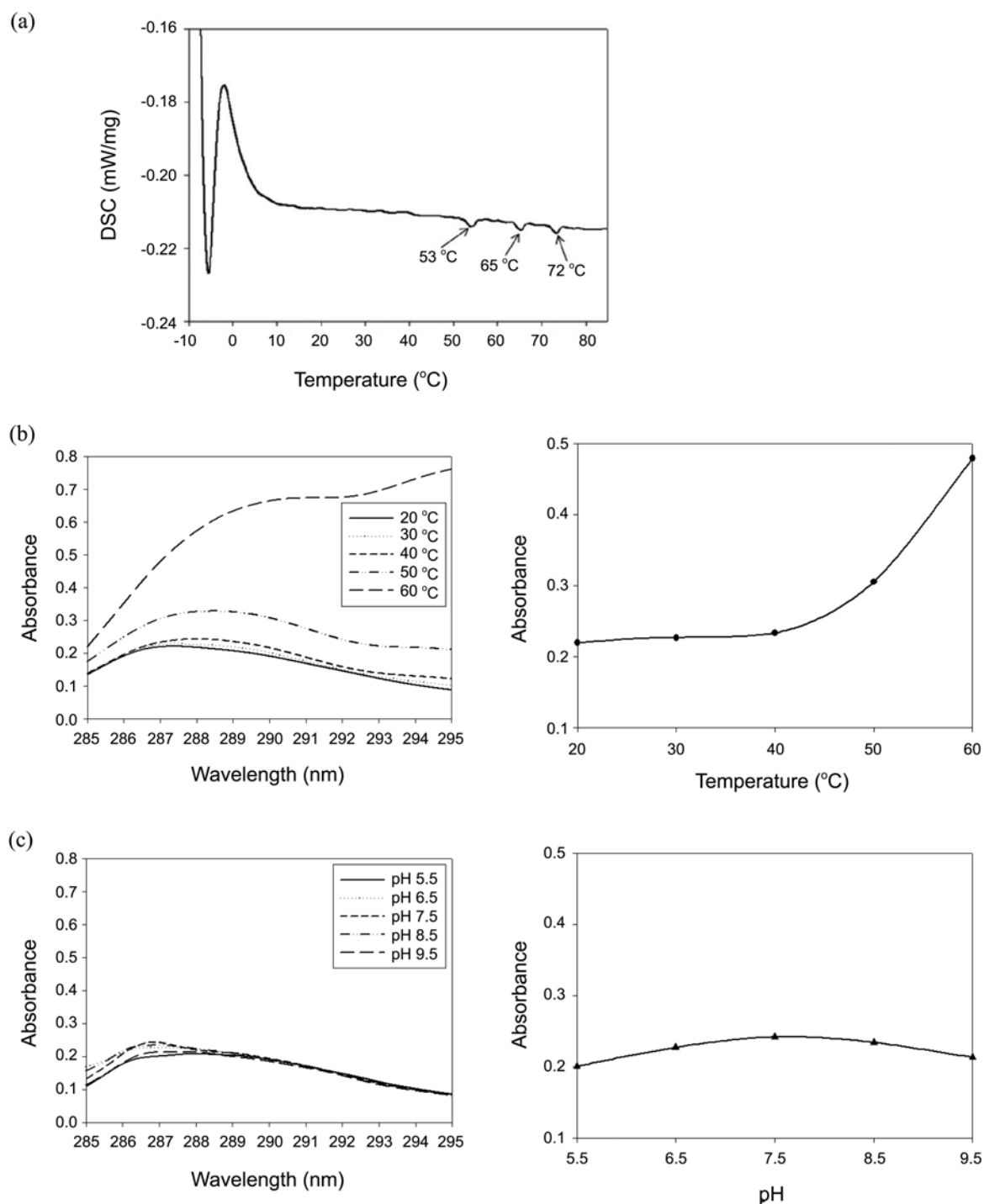


**Figure 4.** (a) Differential scanning calorimetry spectrum of Tl-gal protein. Measurements were carried out on a DSC 204 F1 (NETZSCH DSC, USA). (b, c) Thermal unfoldings of Tl-gal protein were measured by UV-vis spectrophotometer. Absorbances were monitored in the 285-295 nm range under various temperatures and pH (left panel). Absorbance changes were recorded at the wavelength of 287 nm (right panel).

described in Methods section, the overexpressed proteins were purified by Ni-NTA affinity and gel-filtration chromatographies. After high-performance gel chromatography, the concentration of Tl-gal in each fraction was determined using the Bradford method. All purification steps were analyzed by SDS-PAGE and Coomassie blue staining as shown in Figure 2. The full-length Tl-gal appeared as a single band with a molecular weight of 32 kDa (7 mg/mL). MALDI-TOF MS analysis revealed the approximate molecular mass was in accordance with the theoretical mass prediction for the Tl-gal protein. The protein was identified as 32 kDa beta-galactoside-binding lectin lec-3 (Parasite, Mw 31.403, score 129).

The folding property of the Tl-gal protein was characterized by CD spectroscopy. To determine the nature of the secondary structural elements of Tl-gal, far-UV CD spectra were recorded and analyzed. The CD spectra of Tl-gal contained one negative maximum at 215 nm. The CD signal was converted to mean residue ellipticity (MRE) using the following equation:  $MRE = \theta / (10 \cdot l \cdot C \cdot N_A)$ , where  $\theta$  is the ellipticity in mdeg,  $l$  is the light pathlength in cm,  $C$  is the molar concentration of the protein, and  $N_A$  is the number of protein residues. The conformational changes of the Tl-gal protein were dependent on temperature and almost independent of pH (Figs. 3 and 4). In other words, Tl-gal protein was stable at low temperature below 40 °C and various pH conditions. At temperatures above 50 °C, large structural changes in Tl-gal were observed relative to low temperature. *Leishmania* parasites are highly adaptable to different environment pH values, as demonstrated in various enzymatic assays.<sup>20</sup> Temperature-induced changes in the structure of the parasite were observed by electron microscopy.<sup>21</sup>

Differential scanning calorimetry was used to analyze the effects of heat on protein stability. DSC scans were performed under conditions where the protein was irreversibly unfolded. In this study, the thermal transitions or denaturation of the protein was evaluated from -10 °C up to 90 °C. Tl-gal showed three endothermic peaks ( $T_d$ ) at 53, 65, and 72 °C (Fig. 4(a)). This result demonstrates that different conformational changes in Tl-gal occurred in response to changes in temperature. Conformational changes in Tl-gal were also observed in the CD spectra analysis at temperatures above 50 °C. Thermal unfolding experiments of Tl-gal protein using a UV-vis spectrophotometer also support the thermal behavior with CD and DSC results. The thermal denaturation result is based on the exposition of some aromatic residues buried within the hydrophobic core of the protein to the solvent during unfolding. This destabilizes the protein molecule and enhances the formation of intermolecular  $\beta$ -sheet. The absorbance change of the Tl-gal protein on temperature and pH suggests a structural change on temperature and a negligible pH effect (Figs. 4(b) and 4(d)).

Tl-gal protein crystals were grown using a reservoir of 30% polyethylene glycol-400 with 0.1 M CHES buffer at pH 9.5. The crystals grew as a single crystal with typical

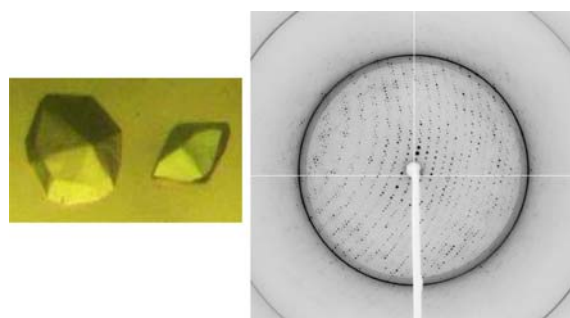


**Figure 5.** Crystals and diffraction pattern of Tl-gal protein.

dimensions of  $100 \times 100 \times 30 \mu\text{m}$  (Fig. 4). Crystal was transferred to the same buffer and a single crystal was picked up using a mounted cryoloop for data collection. The diffraction data was collected with a resolution of 3.0 Å at 100 K. A total of 294,380 measured reflections were merged into 24,478 unique reflections with an  $R_{\text{merge}}$  (on intensity) of 8.7%. The merged data set was 80.3% complete with a resolution of 3.0 Å (Table 1). The crystal belongs to the tetragonal space group  $P4_1$  with unit cell dimensions  $a = b = 75.70$ ,  $c = 248.38$  Å. The asymmetric unit contained four molecules of Tl-gal, giving a crystal volume per protein mass ( $V_m$ ) of  $2.8 \text{ \AA}^3 \text{ Da}^{-1}$  with a solvent fraction of 54.1%. Table 1 summarizes the statistics for the data collection.

We found two structurally conserved protein domains of Tl-gal. The EXPASY search results combined with the PDB revealed considerable sequence similarity between full-length Tl-gal and 3 reference proteins [human galectin-7 (1BKZ), human galectin-8 (3NAJ) and human galectin-9 (3NV1)]. The N domain of Tl-gal (aa 1-143) showed 32% sequence identity with the human galectin-7 (aa 1-135). The C domain of Tl-gal (aa 144-278) showed 40% sequence identity with the human galectin-9 (aa 188-323). Full-length human galectin-9 structure has not been determined yet. The full-length of Tl-gal (aa 1-278) showed 28% sequence identity with the human galectin-8 (aa 1-317). We are planning to use molecular replacement or the multiple isomorphous replacement method to solve the structure.

In the present study, we evaluated the biophysical features, crystallization behavior, and crystallographic properties of the Tl-gal protein in *E. coli*. We are planning to use molecular replacement or multiple isomorphous replacement methods to solve the Tl-gal structure. Tl-gal function will be deduced from the structural analysis. Tl-gal may function as a host galectin-9, thus functioning as a regulatory molecule in the host immune system. Structural information on Tl-gal will be useful in the development of novel therapeutic strategies to treat autoimmune diseases, inflammatory processes and allergic reactions.

**Acknowledgments.** This study was supported by Basic Science Research Program through the National Research Foundation of Korea (NRF) funded by the Ministry of Education, Science and Technology (2011-0026657) to S.B.J and (2011-0026995) to M.S.J. This study was sup-

ported by the Research Fund Program of Research Institute for Basic Sciences, Pusan National University, Korea, 2011, project No. RIBS-PNU-1011-104.

### References

1. Reddy, A.; Fried, B. *Parasitol. Res.* **2007**, *100*, 921-927.
  2. Kim, J. Y.; Cho, M. K.; Choi, S. H.; Lee, K. H.; Ahn, S. C.; Kim, D. H.; Yu, H. S. *Mol. Biochem. Parasitol.* **2010**, *174*, 53-61.
  3. Elliott, D. E.; Summers, R. W.; Weinstock, J. V. *Curr. Opin. Gastroenterol.* **2005**, *21*, 51-58.
  4. Bebb, J. R.; Scott, B. B. *Aliment. Pharmacol. Ther.* **2004**, *20*, 151-159.
  5. Gomez-Escobar, N.; Lewis, E.; Maizels, R. M. *Exp. Parasitol.* **1998**, *88*, 200-209.
  6. Gregory, W. F.; Blaxter, M. L.; Maizels, R. M. *Molecular & Biochemical Parasitology* **1997**, *87*, 85-95.
  7. Yenbutr, P.; Scott, A. L. *Infect Immun.* **1995**, *63*, 1745-1753.
  8. Joseph, G. T.; Huima, T.; Lustigman, S. *Mol. Biochem. Parasitol.* **1998**, *96*, 177-183.
  9. Thomas, P. G.; Carter, M. R.; Atochina, O.; Da'Dara, A. A.; Piskorska, D.; McGuire, E.; Harn, D. A. *Journal of Immunology* **2003**, *171*, 5837-5841.
  10. Murray, J.; Gregory, W. F.; Gomez-Escobar, N.; Atmadja, A. K.; Maizels, R. M. *Mol. Biochem. Parasitol.* **2001**, *118*, 89-96.
  11. Beall, M. J.; McGonigle, S.; Pearce, E. J. *Mol. Biochem. Parasitol.* **2000**, *111*, 131-142.
  12. Rabinovich, G. A.; Baum, L. G.; Tinari, N. *et al. Trends in Immunology* **2002**, *23*, 313-320.
  13. Rubinstein, N.; Ilarregui, J. M.; Toscano, M. A.; Rabinovich, G. A. *Tissue Antigens.* **2004**, *64*, 1-12.
  14. Moore, K. W.; de Waal, M.; Coffman, R. L.; O'Garra, A. *Annu. Rev. Immunol.* **2001**, *19*, 683-765.
  15. Gorelik, L.; Fields, P. E.; Flavell, R. A. *J. Immunol.* **2000**, *165*, 4773-4777.
  16. Chen, W.; Jin, W.; Hardegen, N.; Lei, K. J.; Li, L.; Marinos, N.; McGrady, G.; Wahl, S. M. *J. Exp. Med.* **2003**, *198*, 1875-1886.
  17. Gerald, B. CD spectroscopy deconvolution, version 2.1 **1997**.
  18. Leslie, A. G. W. *Acta Cryst.* **2006**, *D62*, 48-57.
  19. Otwinowski, Z.; Minor, W. *Methods Enzymol.* **1997**, *276*, 307-326.
  20. Zilberstein, D.; Shapira, M. *Annu. Rev. Microbiol.* **1994**, *48*, 449-470.
  21. Pan, A. A.; Pan, S. C. *Exp. Parasitol.* **1986**, *62*, 254-265.
-